Pair entanglement in dimerized spin-s chains

A. Boette, R. Rossignoli, N. Canosa, J. M. Matera

Departamento de Física-IFLP, Universidad Nacional de La Plata,

C.C. 67, La Plata (1900), Argentina

Abstract

We examine the pair entanglement in the ground state of finite dimerized spin s chains interacting through anisotropic XY couplings immersed in a transverse magnetic field, by means of a self-consistent pair mean field approximation. The approach, which makes no a priori assumptions on the pair states, predicts, for sufficiently low coupling between pairs, $2s$ distinct dimerized phases for increasing fields below the pair factorizing field, separated by spin parity breaking phases. The dimerized phases lead to approximate magnetization and pair entanglement plateaus, while the parity breaking phases are characterized by weak pair entanglement but non-negligible entanglement of the pair with the rest of the system. These predictions are confirmed by the exact results obtained in finite $s = 1$ and $s = 3/2$ chains. It is also shown that for increasing values of the spin s, the entanglement of an isolated pair, as measured by the negativity, rapidly saturates in the anisotropic XY case but increases as $s^{1/2}$ in the XX case, reflecting a distinct single spin entanglement spectrum.

PACS numbers: 03.65.Ud,03.67.Mn,75.10.Jm,64.70.Tg

I. INTRODUCTION

The study of entanglement in interacting spin systems has received strong attention in recent years [1, 2]. Entanglement has provided a novel perspective for the analysis of correlations and quantum phase transitions [1–3], being also essential for determining the potential of such systems in the field of quantum information [5]. Interest in spin systems has been enhanced by the impressive advances in control techniques of quantum systems [6], that have made it possible to simulate interacting spin models with different type of couplings by means of trapped ions, Josephson junctions and cold atoms in optical lattices [7–12].

In particular, dimerized systems, characterized by strongly coupled spin pairs and arising from various possible geometric configurations and couplings [13–26], are of great interest, providing a basis for understanding magnetization plateaus and non-trivial magnetic behavior [26]. They have also been recently simulated with cold atoms in optical lattices [27]. While the basic case deals with singlet pairs in antiferromagnetic (AFM)-like systems [25], other types of dimerization can also arise in the ground state (GS) of systems with non-uniform couplings, like spin chains with alternating-type XYZ couplings [13–15, 19, 22–25]. In these systems a basic mean field approximation (MF) based on independent spins clearly fails to provide even the most basic features of the GS and its magnetic behavior. Instead, we have shown [24] that a pair MF approach, a particular case of a generalized cluster-type variational mean field treatment, based on independent pairs whose state is self-consistently determined and admitting relevant symmetry-breaking, is able to provide a correct basic description. In dimerized spin 1/2 arrays with anisotropic XY and XYZ couplings the approach is in fact analytic, providing a phase diagram that differs from that of the standard MF and contains a (single) dimerized phase at low fields under appropriate conditions [24]. Such prediction is in good agreement with the exact results, which in the special case of spin 1/2 chains with first neighbor XY couplings can be analytically obtained through the Jordan-Wigner fermionization [13, 14, 23, 28].

The aim of this work is to extend previous results to spin s systems with $s \geq 1$, where the previous fermionization is no longer available and where the system Hilbert space dimension becomes rapidly very large for exact numerical solutions as the total number of spins increases. In this scenario we will show that the self-consistent pair MF approach

constitutes a convenient method for understanding the basic physics, which can still depart considerably from the conventional MF prediction and the bosonic-like behavior expected for high spin [29]. The approach also provides an accurate description of the reduced state of pairs, enabling to determine the main features of the pair entanglement. In particular, for sufficiently low coupling and appropriate anisotropies, the approach predicts $2s$ dimerized phases for increasing fields below the factorizing field [30], characterized by magnetization and pair entanglement approximate plateaus, which are separated by S_z parity breaking phases where the pair entanglement drops considerably while that of the pair with the remaining chain becomes non-negligible. These features are confirmed by the exact numerical results obtained in small finite spin 1 and 3/2 chains. We will also analyze the behavior for large spin, showing the distinct entanglement properties of anisotropic XY and XX pairs. The formalism and its application to dimerized spin s XY systems is described in sec. II, while results are discussed in detail in sec. III. Conclusions are given in IV.

II. FORMALISM

A. Pair mean field in dimerized arrays and parity breaking

We consider a finite chain of $2n$ spins s in a transverse uniform field B interacting through alternating first neighbor anisotropic XY couplings [13–15, 22, 23], such that the chain contains strongly coupled pairs weakly interacting with their neighboring pairs. The Hamiltonian can be written as

$$H = \sum_{i=1}^{n} [B(S^z_{2i-1} + S^z_{2i}) - \sum_{\mu=x,y} J_\mu (S^\mu_{2i-1} S^\mu_{2i} + \alpha S^\mu_{2i} S^\mu_{2i+1})] \,, \tag{1}$$

where S^μ_i are the spin components at site i (with $S^\mu_{2n+1} = S^\mu_1$ (0) in the cyclic (open) case), J_μ are the exchange couplings and the parameter α indicates the relative strength of the coupling between pairs ($|\alpha| \leq 1$). Without loss of generality we can assume (for even n in the cyclic case) $\alpha \geq 0$ and $J_x \geq 0$, as their signs can be changed by local rotations around the z axis. We can obviously also set $B \geq 0$ (its sign is changed by a global rotation around the y axis) and $|J_y| \leq J_x$. The relevant symmetry for $J_y \neq J_x$ is the S^z parity $P_z = \exp[\imath 2\pi \sum_{i=1}^{2n} (S^z_i + s)] = \prod_{i=1}^{2n} P_{zi}$, which satisfies $[P_z, H] = 0$.

In a pair mean field (MF) treatment, the GS of (1) is approximated by a pair product state $|\Psi_0\rangle = \prod_{i=1}^{n} |\psi_{0i}\rangle$, with $|\psi_{0i}\rangle$ the state of the pair $(2i-1, 2i)$. Minimization of $E_0 =$

$\langle\Psi_0|H|\Psi_0\rangle$ then leads to the independent pair self-consistent Hamiltonian $h=\sum_{i=1}^{n}h_i$, with

$$h_i = B(S^z_{2i-1}+S^z_{2i}) - \sum_\mu J_\mu[S^\mu_{2i-1}S^\mu_{2i} + \alpha(S^\mu_{2i}\langle S^\mu_{2i+1}\rangle + \langle S^\mu_{2i-2}\rangle S^\mu_{2i-1})]\,, \tag{2}$$

where $\langle S^\mu_{2i+j}\rangle = \langle\psi_{0i}|S^\mu_{2i+j}|\psi_{0i}\rangle$, $i=1,\ldots,n$, $j=-1,0$, are the mean values in the GS $|\psi_{0i}\rangle$ of h_i (*self-consistency conditions*). The internal coupling of the pair is treated *exactly*. The energy is then $E_0=\sum_{i=1}^{n}[\langle h_i\rangle + \alpha\sum_\mu J_\mu\langle S_{2i}\rangle\langle S_{2i+1}\rangle]$.

In the ferromagnetic (FM) setting considered, we may assume in the cyclic case a uniform pair mean field such that $\langle S^\mu_{2i-1}\rangle = \langle S^\mu_{2i}\rangle \equiv \langle S^\mu\rangle$ independent of i (unbroken translational symmetry), with $\langle S^y\rangle = 0$ for the lowest energy mean field if $|J_y|<J_x$. Hence, the pair mean field will be characterized by a single parity breaking order parameter $\langle S^x\rangle$: If $\langle S^x\rangle = 0$ it leads to a parity preserving *dimerized phase* at the pair MF level, with no average coupling between pairs, while if $\langle S^x\rangle \neq 0$ it corresponds to a *parity breaking phase*, with non-zero coupling between pairs. This last phase is, of course, twofold degenerate for $|J_y|<J_x$, as both signs $\langle S^x\rangle = \pm|\langle S^x\rangle|$ are equally possible, with $|\psi^-_{0i}\rangle = P_{zi}|\psi^+_{0i}\rangle$. At the parity breaking phases we will then consider the definite parity combinations

$$|\Psi_{0\pm}\rangle \propto (\mathbb{1}\pm P_z)\prod_{i=1}^{n}|\psi^+_{0i}\rangle = \prod_{i=1}^{n}|\psi^+_{0i}\rangle + \prod_{i=1}^{n}|\psi^-_{0i}\rangle\,, \tag{3}$$

satisfying $P_z|\Psi_{0\pm}\rangle = \pm|\Psi_{0\pm}\rangle$, selecting that of lower energy. These states lead to a finite entanglement between pairs.

In order to determine the onset of parity-breaking, we may consider the first order expansion of the common pair ground state $|\psi_0\rangle = |\psi_{0i}\rangle$ for small $\langle S^x\rangle$, $|\psi_0\rangle \approx |\psi^0_0\rangle + |\delta\psi_0\rangle$, where $|\delta\psi_0\rangle = \alpha J_x\langle S^x\rangle\sum_{k>0}\frac{\langle\psi^0_k|S^x_t|\psi^0_0\rangle}{E_k-E_0}|\psi^0_k\rangle$, with $S^x_t = S^x_1+S^x_2$ and $\{|\psi^0_k\rangle\}$ the eigenstates of the $\langle S^x\rangle = 0$ pair Hamiltonian h^0: $h^0|\psi^0_k\rangle = E_k|\psi^0_k\rangle$. Since pair parity symmetry, exactly conserved in h^0, implies $\langle\psi^0_0|S^x_t|\psi^0_0\rangle = 0$ (assuming $|\psi^0_0\rangle$ non-degenerate) we have $\langle S^x\rangle \approx \mathrm{Re}[\langle\psi^0_0|S^x_t|\delta\psi_0\rangle]$ up to first order in $\langle S^x\rangle$, implying the critical condition

$$1 = \alpha J_x\sum_{k>0}\frac{|\langle\psi^0_k|S^x_t|\psi^0_0\rangle|^2}{E_k-E_0}\,. \tag{4}$$

Parity breaking is then feasible if

$$\alpha > \frac{1}{J_x\sum_{k>0}\frac{|\langle\psi^0_k|S^x_t|\psi^0_0\rangle|^2}{E_k-E_0}}\,. \tag{5}$$

Eq. (4) determines a *finite* threshold value for α whenever the isolated pair is *gapped* ($E_k - E_0 > 0\ \forall\ k>0$), which will depend on the relative field strength B/J_x, the ratio $\chi = J_y/J_x$

and the spin s. The sum in (4) is typically exhausted by the first term $\frac{|\langle\psi_1^0|S_t^x|\psi_0^0\rangle|^2}{E_1-E_0}$ with E_1 the lowest energy of S^z parity opposite to that of E_0. We also have the restriction $\alpha \leq 1$, which sets an upper bound on B/J_x ($B < B_c^p$).

On the other hand, the threshold value *vanishes* when the smallest excitation energy $E_1 - E_0$ becomes zero. Hence, pair GS level crossings will separate distinct dimerized phases at sufficiently low α, leading to several onsets (and "deaths") of parity breaking as the field increases, as shown in the next section. For $s = 1/2$ there are [24] two parity preserving phases if $\chi > 0$ and $\alpha < \frac{1}{2}\chi$, with parity breaking in a *single* field window $B_{c1} < B < B_{c2}$.

Such multiple dimerized phases are obviously absent in the conventional single spin MF (full product state approximation), which in this system becomes equivalent to the MF treatment of a standard chain with uniform coupling of strength $J_x(1+\alpha)/2$, being independent of J_y if $|J_y| < J_x$. For any spin s it leads to a single parity breaking phase for $|B| < B_c^{\rm mf} \equiv J_x s(1+\alpha)$, where $\langle S_x\rangle = \pm s \sin\theta$ with $\cos\theta = B/B_c^{\rm mf}$.

Nevertheless, for $0 < J_y < J_x$ there is one point where *both* the single spin and pair mean field treatments coincide and become rigorously *exact* for *any* value of the spin s and the number n of spins, i.e., where the chain GS completely forgets its dimerized structure, which is the *factorizing field* [23, 24]

$$B_s = J_x s(1+\alpha)\sqrt{\chi}\,, \quad \chi = J_y/J_x\,. \tag{6}$$

At this field the chain exhibits a pair of degenerate *completely separable* parity breaking aligned ground states

$$|\pm\Theta\rangle = |\pm\theta, \pm\theta, \ldots\rangle\,, \tag{7}$$

with $|\pm\theta\rangle = e^{\mp i\theta S^y}|-s\rangle$ a single spin state with maximum spin forming an angle $\pm\theta$ with the $-z$ axis, with $\cos\theta = B_s/B_c^{\rm mf} = \sqrt{\chi}$. In a finite chain the factorizing field (6) is actually that where the *last* GS parity transition takes place[33, 34] (see next section). Accordingly, the side-limits of the exact GS at B_s in a finite chain will not be given by the product states (7) but rather by the definite parity combinations $|\Theta_\pm\rangle \propto |\Theta\rangle \pm |-\Theta\rangle$, with $P_z|\Theta_\pm\rangle = \pm|\Theta_\pm\rangle$ [33, 34], which will then be correctly predicted by the symmetry-restored pair MF states (3). A GS transition $|\Theta_-\rangle \to |\Theta_+\rangle$ will then take place as B crosses B_s.

For AFM type couplings ($J_x < 0$ and/or $\alpha < 0$ in (1)), factorizing and critical values of B and α take exactly the same previous values. Just suitable local rotations are to be applied to the corresponding state. For instance, if $J_x > 0$ but $\alpha < 0$, they will transform

the previous uniform pair state into a Neel type pair state $|\Psi_0\rangle = |\psi_0\rangle|\tilde{\psi}_0\rangle|\psi_0\rangle\ldots$ with $|\tilde{\psi}_0\rangle = e^{-i\pi(S_1^z+S_2^z)}|\psi_0\rangle \propto P_z|\psi_0\rangle$ and $\langle S^x\rangle_{2i+j} = (-1)^{i-1}\langle S^x\rangle$ for $j = 0, -1$. These rotations will not affect the energy spectrum nor entanglement measures.

The pair MF approach can of course be applied to more complex couplings and geometries. For instance, if the coupling between pairs i and $i+1$ contains second and third neighbor terms, such that it is of the form $-\sum_\mu J_\mu \sum_{j,l=1,2} \alpha_{jl} S^\mu_{2i-2+j} S^\mu_{2i+l}$ we should just replace the α-term in (2) by $\sum_{j,l=1,2} S^\mu_{2i-2+j}(\alpha_{jl}\langle S^\mu_{2i+l}\rangle + \alpha_{lj}\langle S^\mu_{2i-4+l}\rangle)$. If translational symmetry remains unbroken, as will occur for $\alpha_{jl} \geq 0\ \forall\ j, l$, previous equations can be directly applied, leading to the same critical condition (4) with $\alpha = \sum_{j,l=1,2} \alpha_{j,l}$. For different signs, the possibility of non-uniform solutions should also be considered.

B. Entanglement

The reduced state of a strongly coupled pair in the exact GS $|\Psi_0\rangle$ of the chain is given by $\rho_{12} = \mathrm{Tr}_{3,4,\ldots}|\Psi_0\rangle\langle\Psi_0|$. The entanglement of the pair with the rest of the chain can be measured through the entanglement entropy $S(\rho_{12}) = -\mathrm{Tr}\rho_{12}\log_2\rho_{12}$, satisfying $S(\rho_{12}) \leq 2\log_2(2s+1)$ for a pair of spins s. On the other hand, its internal entanglement can be estimated through the negativity (an entanglement monotone computable for mixed states of any dimension [31, 32])

$$N_{12} = (\mathrm{Tr}\,|\rho_{12}^{t_2}| - 1)/2\,, \tag{8}$$

where ρ^{t_2} denotes the partial transpose of ρ_{12}. Eq. (8) is just minus the sum of the negative eigenvalues of $\rho_{12}^{t_2}$. If ρ_{12} is pure ($\rho_{12} = |\psi_0\rangle\langle\psi_0|$) Eq. (8) becomes a generalized entanglement entropy,

$$N_{12} = [(\mathrm{Tr}\,\sqrt{\rho_1})^2 - 1]/2 = \sum_{i<j} \lambda_i^1\lambda_j^1 \tag{9}$$

where $\rho_1 = \mathrm{Tr}_2\,|\psi_0\rangle\langle\psi_0|$ is the single spin reduced state and λ_i^1 its eigenvalues. Accordingly, Eq. (9) vanishes for ρ_1 pure ($|\psi_0\rangle$ separable) and reaches its maximum for a maximally mixed ρ_1 ($|\psi_0\rangle$ maximally entangled), in which case $N_{12} = s$ for a pair of spins s.

At the pair MF level, ρ_{12} will be pure in the parity preserving phases. However, in the parity breaking phases ρ_{12} will become *mixed* if the parity restored states (3) are employed. The latter lead to a rank 2 reduced state of the form

$$\rho_{12} \approx \frac{1}{2}(|\psi_0^+\rangle\langle\psi_0^+| + |\psi_0^-\rangle\langle\psi_0^-|)\,, \tag{10}$$

if the complementary overlap $|\langle\psi_0^+|\psi_0^-\rangle|^{n-1}$ (negligible if n and $\langle S^x\rangle$ are not too small) is discarded, whose non-zero eigenvalues are just $\lambda_\pm = \frac{1}{2}(1 \pm |\langle\psi_0^-|\psi_0^+\rangle|)$. Hence, a non-zero entanglement entropy of the pair with the rest of the chain will arise at the pair MF level within the parity breaking phases, which will then satisfy $S(\rho_{12}) \leq 1$, with $S(\rho_{12}) \approx 1$ if the overlap $\langle\psi_0^-|\psi_0^+\rangle$ is also negligible.

At the factorizing field (6), Eq. (10) becomes *exact* (if $\langle -\theta, -\theta|\theta, \theta\rangle^{n-1} = (\cos^{4s}\theta)^{n-1}$ is neglected), with $|\psi_0^\pm\rangle = |\pm\theta, \pm\theta\rangle$ product states. Consequently, even with symmetry restoration the exact side-limits of ρ_{12} at B_s will become *separable*, i.e. a convex combination of product states [35], leading to $N_{12} = 0$ at this point. Nonetheless, it will remain *mixed*, with eigenvalues $\lambda_\pm = \frac{1}{2}(1 \pm \cos^{4s}\theta)$, implying a nonzero entanglement of the pair with the rest of the chain at the side-limits $B \to B_s^\pm$.

III. RESULTS

A. The spin-1 case

1. *The spin 1 pair*

We first examine in detail the case $s = 1$. In order to understand the behavior of both the pair MF and the exact solution for general α in (1), we first discuss the isolated pair ($\alpha = 0$). The lowest energy levels of the pair for each parity P_z and for $|J_y| \leq J_x$ are

$$E_+ = -\sqrt{2B^2 + \tfrac{J_x^2+J_y^2}{2} + \sqrt{4B^2(B^2 - J_xJ_y) + \tfrac{(J_x^2+J_y^2)^2}{4}}}\,, \tag{11}$$

$$E_- = -[\tfrac{J_x+J_y}{2} + \sqrt{B^2 + \tfrac{(J_x-J_y)^2}{4}}]\,, \tag{12}$$

with eigenstates

$$|\psi_+\rangle = \alpha_-|-1,-1\rangle + \alpha_0|0,0\rangle + \alpha_+|1,1\rangle + \alpha_{11}\tfrac{|-1,1\rangle+|1,-1\rangle}{\sqrt{2}}\,, \tag{13}$$

$$|\psi_-\rangle = \beta_-\tfrac{|-1,0\rangle+|0,-1\rangle}{\sqrt{2}} + \beta_+\tfrac{|0,1\rangle+|1,0\rangle}{\sqrt{2}} = \tfrac{|0,\phi\rangle+|\phi,0\rangle}{\sqrt{2}}\,, \tag{14}$$

in the standard product basis $\{|m_1, m_2\rangle\}$ of eigenstates of S_1^z and S_2^z, where

$$\alpha_0 = \alpha_-\tfrac{2(|E_+|-2B)}{J_x-J_y},\quad \alpha_+ = \alpha_-\tfrac{|E_+|-2B}{|E_+|+2B},\quad \alpha_{11} = \alpha_0\tfrac{J_x+J_y}{\sqrt{2}|E_+|}$$
$$\beta_+ = \beta_-\tfrac{2(|E_-|-B)-(J_x+J_y)}{J_x-J_y}\,. \tag{15}$$

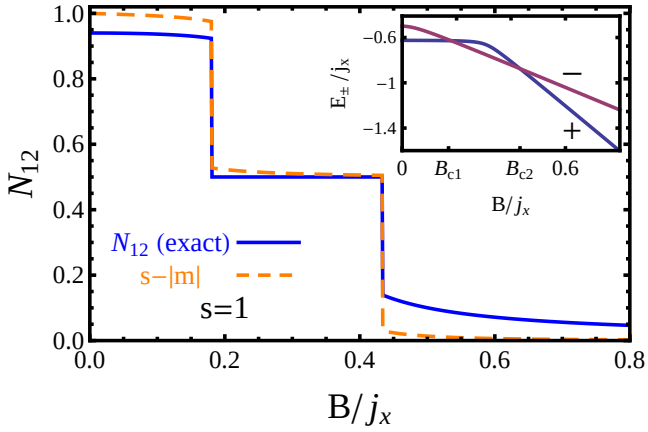

FIG. 1. (Color online) Negativity of the spin 1 pair GS for an anisotropic XY coupling with $\chi = J_y/J_x = 0.75$, as a function of the scaled transverse field B/j_x, with $j_x = 2J_x s$. The quantity $s - |m|$, with m the intensive magnetization $\langle S_1^z + S_2^z\rangle/2$, is also depicted. The inset depicts the lowest energy levels $E_\pm$ for each parity, which cross at B_{c1} and $B_{c2} = B_s$ (pair separability field) and lead to the negativity steps (all labels dimensionless in all figures).

Here $|\psi_-\rangle$ is seen to be a Bell type state, with $|\phi\rangle = \beta_-|-1\rangle + \beta_+|1\rangle$, whereas $|\psi_+\rangle$ has full Schmidt rank if $J_y \neq J_x$. For strong fields $B \gg J_x$, $E_+ \approx -2B$, $E_- \approx -B$, while for zero field $E_+ = -J_x\sqrt{1+\chi^2}$, $E_- = -J_x$, so that $|\psi_+\rangle$ is the GS in these limits. Yet if $\chi = J_y/J_x \in (0,1]$, $|\psi_-\rangle$ will be the GS in an intermediate field window $B_{c1} \leq B \leq B_{c2}$, as seen in the inset of Fig. 2, with

$$B_{c1} \approx \sqrt{\chi} J_x \tfrac{(1-4\chi/25)}{\sqrt{5}}, \quad B_{c2} = \sqrt{\chi} J_x = B_s\,, \tag{16}$$

where the expression for B_{c1} holds for small χ and B_s is the *separability field* (6) for the isolated pair ($\alpha = 0$). Hence, for $\chi > 0$ the pair GS will undergo two parity transitions as the field increases from 0, the last one at B_s. These transitions are reminiscent of the magnetization transitions $M \to M-1$ for $M = 0, 1$ of the XX case $J_y = J_x$ ($\chi = 1$), where the eigenvalue M of $S_t^z = S_1^z + S_2^z$ is a good quantum number and $B_{c1} = (\sqrt{2}-1)J_x$, $B_s = J_x = B_c^{\rm mf}$. Accordingly, in the XX case the eigenstates (13)–(14) become $|\psi_+\rangle = \frac{1}{\sqrt{2}}(\frac{|-1,1\rangle+|1,-1\rangle}{\sqrt{2}} + |0,0\rangle)$ for $|B| < B_{c1}$ and $|-1,-1\rangle$ for $B > B_s$, with $|\psi_-\rangle = \frac{|-1,0\rangle+|0,-1\rangle}{\sqrt{2}}$. Here GS separability holds $\forall\ B \geq B_s$.

In both the XY and XX cases, these GS transitions lead to a stepwise decrease of the pair entanglement, which parallels that of $s-|m|$, with $m = \langle S_t^z\rangle/2$ the intensive magnetization, as appreciated in Fig. 1. Since $|\psi_-\rangle$ is a Bell type state, it has a *fixed* entanglement entropy

$S_{12} = 1$ and negativity $N_{12} = 1/2$, independent of the anisotropy and field intensity (strict entanglement plateau). On the other hand, $|\psi_+\rangle$ in (13) leads to a larger negativity for $|B| < B_{c1}$, not strictly constant, given at zero field by

$$N_{12} = \frac{1 + |\chi|(1 + |\chi| + \chi^2 + \sqrt{1+\chi^2})}{2\sqrt{(1+\chi^2)^3}}\,. \tag{17}$$

This value increases with $|\chi|$ for $|\chi| \leq 1$, reaching $N_{12} = \frac{1}{4} + \frac{1}{\sqrt{2}} \approx 0.96$ at $\chi = 1$ (close to the maximum value $N_{12}^{\max} = 1$ for a spin 1 pair). In contrast, for strong fields $|B| > B_s$ the state (13) becomes almost aligned, with just α_- remaining significant, implying a small negativity $N_{12} \approx \frac{J_x(1-\chi)}{4B}$. As previously stated, it is clearly seen that the side limits of the GS at the pair factorizing field $B_{c2} = B_s$ are the entangled states $|\psi_\pm\rangle$, which at this point become linear combinations of the separable states $|\pm\theta, \pm\theta\rangle$ (Eq. (7)).

The average magnetization $\langle S_t^z \rangle$ is given by $\beta_+^2 - \beta_-^2 = \frac{-B}{\sqrt{B^2 + J_x^2(1-\chi)^2/4}}$ in $|\psi_-\rangle$, which is close to -1 in the sector where it is GS, and by $\alpha_+^2 - \alpha_-^2$ in $|\psi_+\rangle$, becoming $\approx -\frac{B(1-\chi)^2}{J_x(1+\chi^2)^{3/2}}$ for weak fields $|B| < B_{c_1}$ and $\approx \frac{J_x^2(1-\chi)^2}{8B^2} - 2$ for strong fields $B > B_s$. Hence, the behavior of $s - |m|$ resembles that of the negativity, with $s - |m| \approx N_+^2$ for strong fields.

2. The spin 1 chain

Returning now to the coupled spin 1 chain, the previous GS transitions of the isolated pair will imply three distinct dimerized phases if $\chi > 0$ and α is sufficiently small, as appreciated in the pair MF phase diagram depicted in Fig. 2. For fixed $B < B_c^p \approx J_x s$, Eq. (5) determines the threshold value $\alpha_c(B)$ for parity breaking, which vanishes precisely at the critical fields B_{c1} and B_{c2} of the isolated pair. For $\alpha < \alpha_c(B)$ we then obtain a *dimerized phase* in this approach, with all strongly coupled pairs in a strongly entangled state $|\psi_+\rangle$ (Eq. (13)) if $|B| < B_{c1}$ or $|\psi_-\rangle$ (Eq. (14)) if $B_{c1} < B < B_s$, and back to an almost aligned state $|\psi_+\rangle$ if $B > B_s$. As B increases from 0 at fixed small α, the pair MF state can then undergo *four* transitions between definite parity and parity breaking phases or vice versa, as appreciated in Fig. 2. At zero field, Eq. (5) leads to the critical value

$$\alpha_c(0) = \frac{(1+\chi^2)(\sqrt{1+\chi^2}(4+\chi^2) - 4 - 3\chi^2)}{\chi^4}\,, \tag{18}$$

which increases with $|\chi|$, reaching ≈ 0.14 for $|\chi| \to 1$ and vanishing as $\approx \chi^2/8$ for $\chi \to 0$. For $\chi = 0.75$ (Fig. 2), $\alpha_c(0) \approx 0.077$.

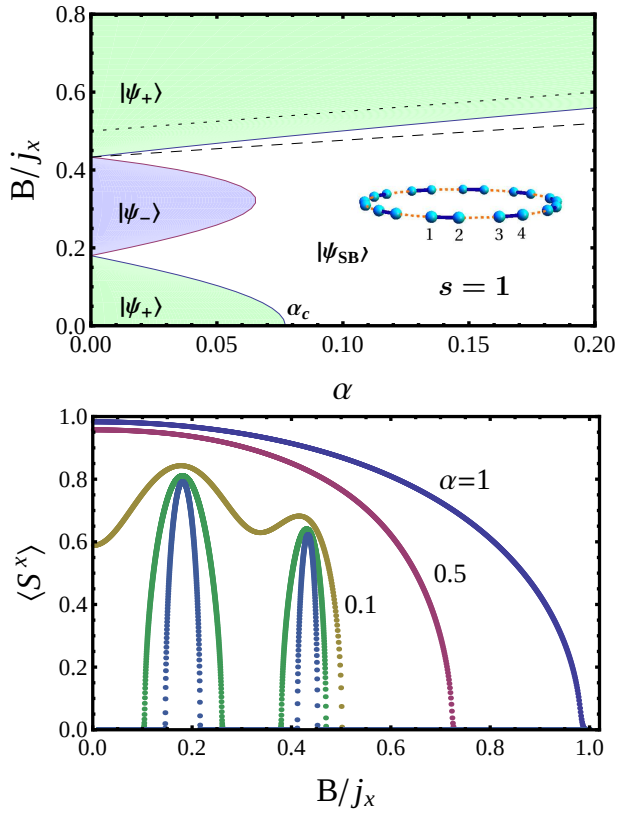

FIG. 2. (Color online) Top: Pair mean field (GMF) phase diagram of the spin 1 dimerized cyclic chain in the α–field plane for $\chi = J_y/J_x = 0.75$. Colored sectors depict dimerized definite S_z parity phases ($\langle S^x \rangle = 0$) whereas the white sector the parity breaking phase (α_c indicates the critical value (18) at zero field). The dashed line depicts the separability field (6), entirely contained in the latter, which determines the last parity transition of the exact GS, while the dotted line the conventional mean field critical field $B_c^{\rm mf} = J_x s(1+\alpha)$. Bottom: The parity breaking parameter $\langle S^x \rangle$ for increasing fields at different fixed α's (0.025,0.05,0.1,0.5 and 1). It's behavior reflects the phases of the top panel, showing a non-monotonous field dependence at low α, with "deaths and revivals" if $\alpha < \alpha_c(0)$. For $\alpha = 1$ it lies close to the conventional mean field result.

On the other hand, if $\alpha > \alpha_c(0)$ we obtain a single parity breaking phase for $|B| < B_c(\alpha)$, with $B_c(\alpha)$ lying between the factorizing field (6) and the standard MF critical field $B_c^{\rm mf}$, as also seen in Fig. 2. In the XX limit $\chi = 1$, $B_s(\alpha) = B_c(\alpha) = B_c^{\rm mf}(\alpha) = J_x$. We also mention that if $\chi < 0$ ($-J_x < J_y < 0$), the isolated pair remains gapped for all fields, with a GS which is always of positive parity and exhibits no sharp transitions. Consequently, in this case parity breaking occurs just above a *finite* threshold $\alpha_c(B) > \alpha_c(0)\ \forall\ B < B_c^p$, i.e.,

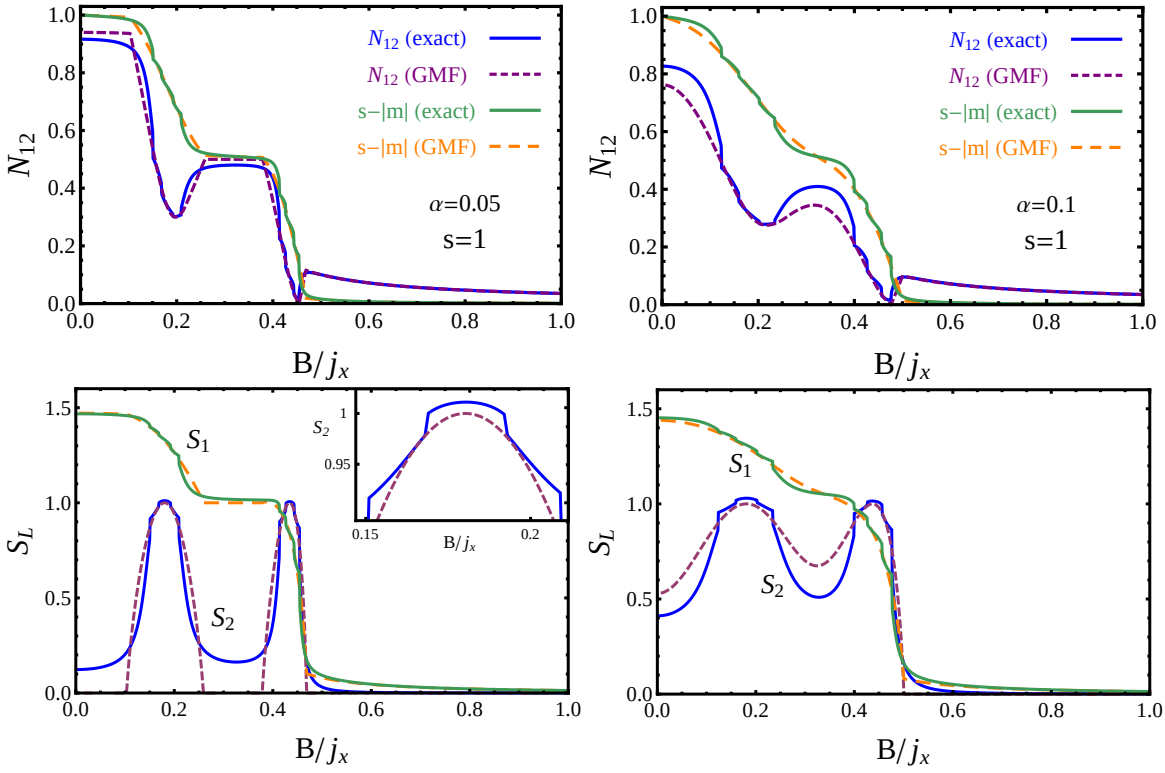

FIG. 3. (Color online) Top panels: Exact and GMF results for the negativity in the dimerized spin 1 chain, as a function of the magnetic field, for coupling factors $\alpha = 0.05$ (left) and $\alpha = 0.1$ (right). The quantity $s - |m|$, with $m = \langle \sum_i S_i^z \rangle / 2n$ the intensive magnetization, is also depicted. Bottom panels: The corresponding exact (solid lines) and GMF (dashed lines) results for the entanglement entropies of a strongly coupled spin pair (S_2) and a single spin (S_1) with the rest of the chain, for the same values of α and s. The inset shows the discontinuities in the exact S_2 stemming from the GS parity transitions, which occur within the parity breaking phases of the GMF approach.

for $\alpha > \alpha_c(0)$ and $|B| < B_c(\alpha) < B_c^{\rm mf}(\alpha)$. If $\alpha < \alpha_c(0)$ and $\chi < 0$ no parity breaking occurs. Thus, we see that the weaker strength J_y does strongly affect the pair MF phase diagram, in contrast with the single spin MF.

Fig. 3 depicts in the top left panel results for the exact negativity of a strongly coupled pair for increasing fields at fixed low α and $\chi = 0.75$, together with the intensive magnetization $m = \langle \sum_i S_i^z \rangle / (2n)$ (through the quantity $s - |m|$), obtained numerically through diagonalization in a small cyclic chain of $2n = 8$ spins. It is first seen that the pair MF pre-

diction, denoted in what follows as GMF (generalized mean field), is in very good agreement with the exact results. The two dimerized phases for $B < B_s$ lead to corresponding approximate plateaus in the negativity N_{12} and magnetization. In the parity breaking phases, N_{12} drops considerably, with the GMF result remaining accurate if evaluated with the parity restored mixed state (10). The vanishing of N_{12} at the factorizing field $B_s \approx 0.44 j_x$ is also appreciated. The behavior of $s-|m|$, on the other hand, is close to that of the pair negativity but exhibits just a straight decrease at the parity breaking sectors, reflecting actually the behavior of the single spin entanglement entropy S_1, shown in the bottom panel.

On the right panels we depict results for $\alpha = 0.1$, for which the definite parity dimerized phases are no longer present in GMF yet the order parameter $\langle S^x \rangle$ still exhibits a non-monotonous evolution with the field magnitude (Fig. 2). Accordingly, the exact results still show a non-monotonous evolution of the negativity, in agreement with the GMF prediction. The magnetization plateaus start to disappear, with m again correctly predicted by GMF.

The magnetic behavior of the entanglement entropies of a strongly coupled spin pair ($S_2 = S(\rho_{12})$) and a single spin ($S_1 = S(\rho_1)$) with the rest of the chain are depicted in the bottom panels. That of S_2 is quite different from S_1, exhibiting peaks at the GMF parity breaking phases or in general at the maxima of the GMF parity breaking parameter $\langle S^x \rangle$, reflecting its behavior. Parity breaking is then directly indicative of the entanglement of the pair with the rest of the chain. Dimerization is also evident through the lower (rather than larger, as in a standard chain) value of S_2 in comparison with S_1 for most fields except in the vicinity of the factorizing field B_s. The behavior of S_1, on the other hand, is qualitatively similar to that of $s - |m|$, since the latter is here an indicator of the mixedness of the reduced state ρ_1 as $\langle S_i^x \rangle = \langle S_i^y \rangle = 0$ due to parity symmetry. The GMF results (obtained with the mixed state (10) in parity breaking phases) are again in good agreement with the exact results for both values of α, providing a clear interpretation and correctly predicting the maximum value $S_2^{\max} \approx 1$ in the parity breaking phases. They also yield the exact side-limits of the these entropies at the factorizing field B_s.

Moreover, the exact GS of the full chain exhibits $2ns$ parity transitions as the field increases from 0 for $\chi > 0$, again reminiscent of the $2ns$ magnetization transitions of the XX chain, with the last one precisely at the factorizing field (6). These transitions *are seen to be confined within the symmetry breaking sectors of the GMF approach*, as appreciated in Fig. 4 and the inset of the bottom left panel in Fig. 3 (they lead to small but appreciable

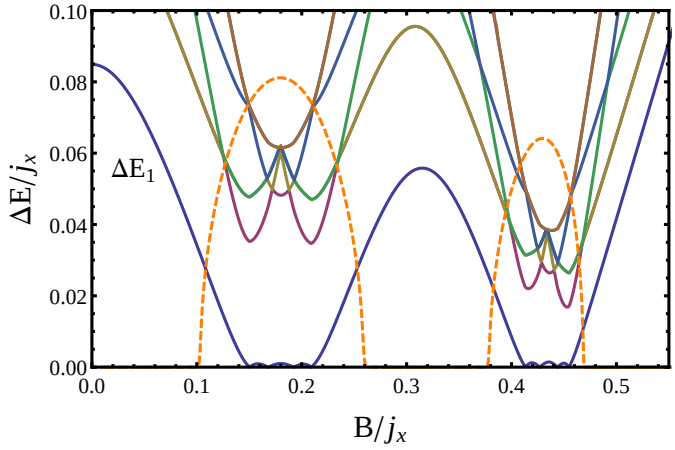

FIG. 4. (Color online) The lowest exact excitation energies in the $2n = 8$ dimerized spin 1 chain for $\alpha = 0.05$. The dashed line depicts the (scaled) GMF parity breaking parameter $\langle S^x \rangle$. All parity transitions of the GS are seen to take place within the GMF parity breaking phases, where the lowest excitation energy becomes small (and the first band of excitation energies minimum).

discontinuities in all depicted quantities for small n). They indicate the crossings of the lowest negative and positive parity exact energy levels, which lie very close in the parity breaking sectors of the pair MF approach, as verified in Fig. 4.

B. Higher Spins

1. *The spin s case*

The general picture remains similar for higher spins s but the number of definite parity dimerized phases at fixed low α arising for $\chi > 0$ and $B < B_s$ in the pair mean field becomes $2s$, following the $2s$ GS parity transitions of the isolated pair for increasing fields (the last one at the factorizing field for the pair, $B_s = J_x s\sqrt{\chi}$). Consequently, there are three of such phases for $s = 3/2$, two of each parity, as seen in Fig. 5 (for easier comparison between different spins, we scaled the fields with $j_x = 2J_x s$ in all Figures, such that B_s/j_x and $B_c^{\rm mf}/j_x = (1+\alpha)/2$ are spin independent, with $B_c^{\rm mf}/j_x = 1$ in the uniform ($\alpha = 1$) chain). For sufficiently small α the pair MF GS can then undergo, for $s = 3/2$, up to six transitions between definite parity and parity breaking phases (or vice versa) as B increases.

It is also seen that the limit value of α for the existence of multiple dimerized phases for

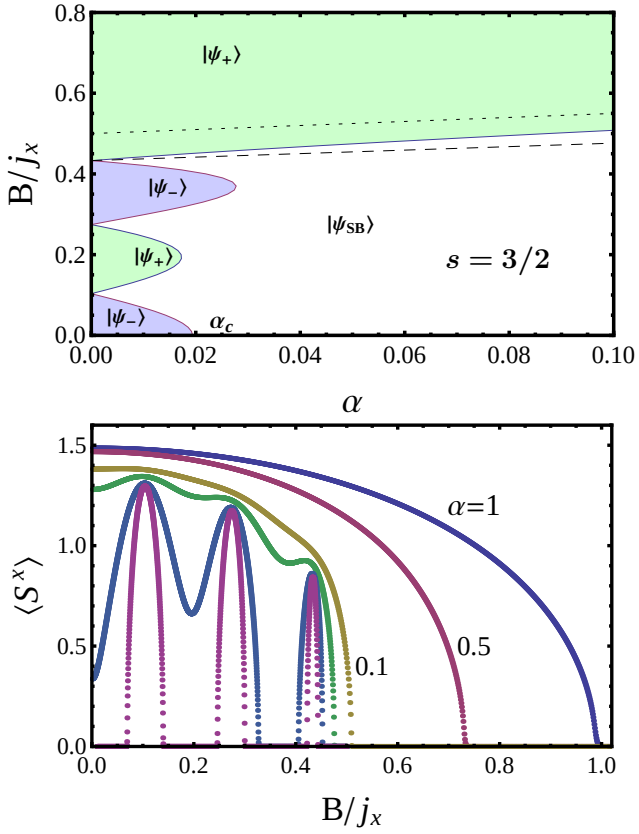

FIG. 5. (Color online) Top panel: The GMF phase diagram of the spin 3/2 dimerized chain in the α-field plane, for anisotropy $\chi = J_y/J_x = 0.75$. There are now three definite parity dimerized phases below B_s (colored sectors) if α is sufficiently small. Remaining details as in Fig. 2. Bottom panel: The corresponding parity breaking parameter $\langle S^x \rangle$ for increasing fields at different fixed values of α ($(0.01, 0.02, 0.05, 0.1, 05$ and $1)$. It's behavior reflects the phases of the top panel, exhibiting a non monotonous variation at low α, with "deaths and revivals" if $\alpha \leq \alpha_c(0)$.

$\chi > 0$ decreases with increasing spin. At zero field, we have essentially $\alpha_c(0) \propto \Delta E/(J_x s^2)$, with $\Delta E = E_1 - E_0$ the energy gap to the first excited state. For $\chi = 1$ (XX case) $\Delta E \propto J_x$ and hence $\alpha_c(0) \propto s^{-2}$. For $s = 3/2$ we obtain in fact $\alpha_c(0) \approx 0.06$. However, for $\chi < 1$ $\alpha_c(0)$ becomes exponentially small for large s, since now ΔE decreases exponentially with increasing spin. The behavior with s of $\alpha_c(B)$ for other fields $B < B_s$ is qualitatively similar. For $\chi = 0.75$ and $s = 3/2$ we obtain $\alpha_c(0) \approx 0.019$, as seen in Fig. 5. Nevertheless, for α above but close to $\alpha_c(0)$ the GMF parity breaking parameter $\langle S^x \rangle$ continues to exhibit a non-monotonous evolution for increasing fields, as seen for $\alpha = 0.05$, where it still has three local minima reminiscent of the dimerized phases. On the other hand, for $\chi < 0$ there is no

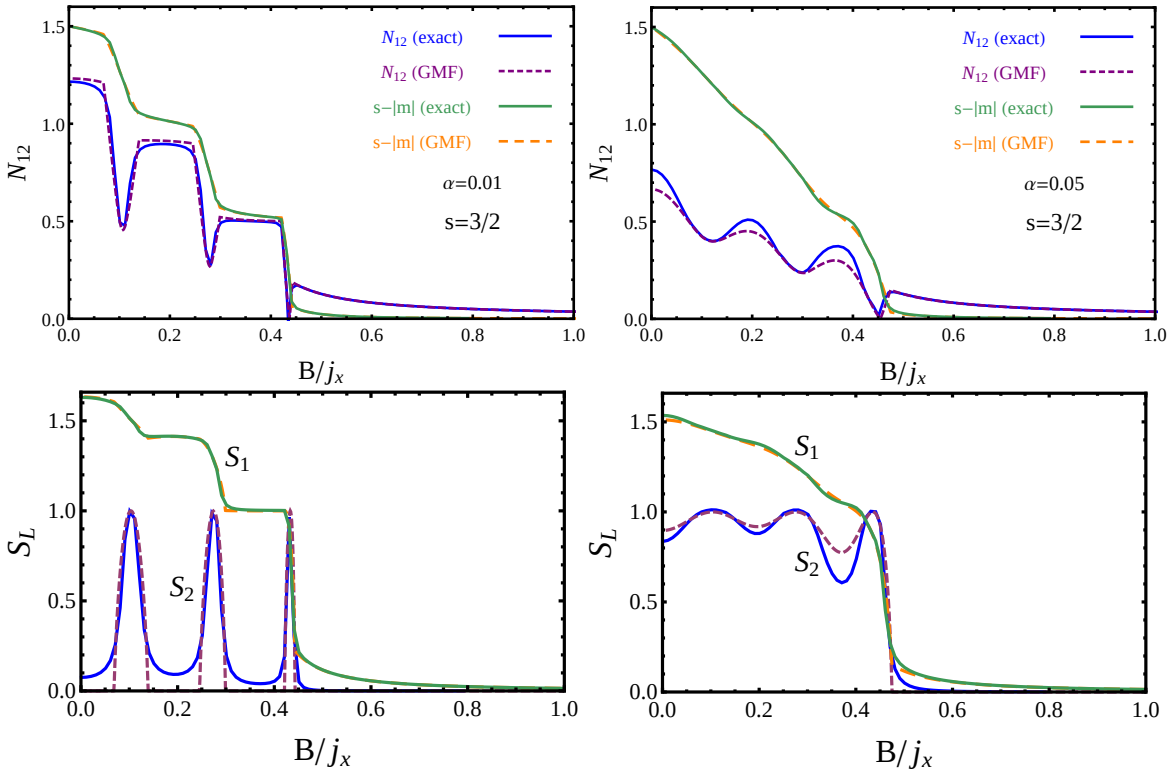

FIG. 6. (Color online) Top: Exact and GMF results for the negativity in the dimerized spin 3/2 chain, as a function of the (scaled) magnetic field, for two different values of the coupling factor α. Again $m = \langle S_z \rangle / n$ denotes the intensive magnetization. Bottom: The corresponding exact (solid lines) and GMF (dashed lines) results for the entanglement entropies of a strongly coupled spin pair (S_2) and a single spin (S_1), with the rest of the chain, as a function of the (scaled) magnetic field in the $s = 3/2$ chain for the previous values of α.

parity breaking if $\alpha < \alpha_c(0)$, as in the $s = 1$ case.

The agreement of the GMF predictions with the exact numerical results remains high at small values of α, as appreciated in Fig. 6. The exact negativity N_{12} and pair entanglement entropy S_2 exhibit, accordingly, a non-monotonous evolution for increasing fields at low α, with N_{12} showing for $\alpha = 0.01$ $2s$ approximate plateaus at the GMF dimerized phases separated by deep valleys at the parity-breaking sectors, before reaching the strong field regime for $B > B_s$. On the other hand, S_2 is again maximum and close to 1 at the center of the parity breaking phases, in full agreement with the GMF result obtained with the parity restored states (10). We also see the $2s$ approximate magnetization plateaus, as predicted by GMF.

These effects become attenuated for $\alpha = 0.05$ (right panels), where the fully dimerized phases for $B < B_s$ no longer exist in GMF, although the behavior of N_{12} and S_2 remains non-monotonous, in agreement with that of $\langle S^x \rangle$ in GMF. It is also seen that the GMF predictions for the magnetization and the single spin entanglement entropy S_1 are very accurate in both panels, with $s - |m|$ a good qualitative indicator of the latter. The exact GS of the finite chain still exhibits $2ns$ parity transitions as B increases from 0, the last one at the factorizing field (6), although the ensuing discontinuities in the depicted quantities become small as s increases. They are again confined to the parity breaking sectors of GMF (i.e., to the narrow parity breaking intervals for $\alpha = 0.01$). As before, factorization at B_s is reflected in the vanishing value of N_{12} at this point, while the entanglement entropies S_1 and S_2 approach the finite limits determined by the corresponding state (10), with $S_2 > S_1$ only in the vicinity of B_s.

2. Behavior for large spin

Let us now examine in more detail the entanglement of a single pair for increasing spin s. In the top panel of Fig. 7 the entanglement spectrum (the eigenvalues of the single spin reduced density matrix ρ_1) is depicted as a function of the applied field for different spins. For $\chi < 1$ the reduced states become essentially rank 2 states as s increases in the whole sector $B < B_s$. The reason is that the main component of the pair GS ($|\psi_+\rangle$ or $|\psi_-\rangle$) is just a parity projected rank 2 mean field state $|\Theta_\pm\rangle$, i.e., $|\psi_\pm\rangle = \gamma|\Theta_\pm\rangle + |\delta\psi_\pm\rangle$, with

$$|\Theta_\pm\rangle = \frac{|\theta,\theta\rangle \pm |-\theta,-\theta\rangle}{\sqrt{2(1 \pm \cos^{4s}\theta)}} = \sqrt{p_\pm}|\theta_+\theta_\pm\rangle + \sqrt{1-p_\pm}|\theta_-\theta_\mp\rangle\,, \tag{19}$$

where the last expression is its Schmidt decomposition, with $|\theta_\pm\rangle = \frac{|\theta\rangle \pm |-\theta\rangle}{\sqrt{2(1\pm\cos^{2s}\theta)}}$ the local orthogonal definite parity states and $p_- = \frac{1}{2}$, $p_+ = \frac{(1+\cos^{2s}\theta)^2}{1-\cos^{4s}\theta}$. These states lead to a rank 2 ρ_1 with eigenvalues $(p_\pm, 1-p_\pm)$. By optimizing the angle θ it is found that the overlap $|\gamma| = |\langle\Theta_\pm|\psi_\pm\rangle|$ exceeds 0.9 for all field and spin values, with $|\langle\Theta_\pm|\psi_\pm\rangle| \gtrsim 0.95$ for all fields if $s \geq 5$. The states (19) become of course the *exact* pair GS at the factorizing field B_s, with the overlap staying above 0.99 for $B > B_s$. We can verify from Fig. 7 that the contribution of $|\delta\psi_\pm\rangle$ to the entanglement spectrum is negligible.

Nonetheless, its contribution to the negativity is important if χ is not too small. For $|B| < B_s$ the states $|\Theta_\pm\rangle$ lead essentially to an almost constant negativity $N_\pm \approx 1/2$ for

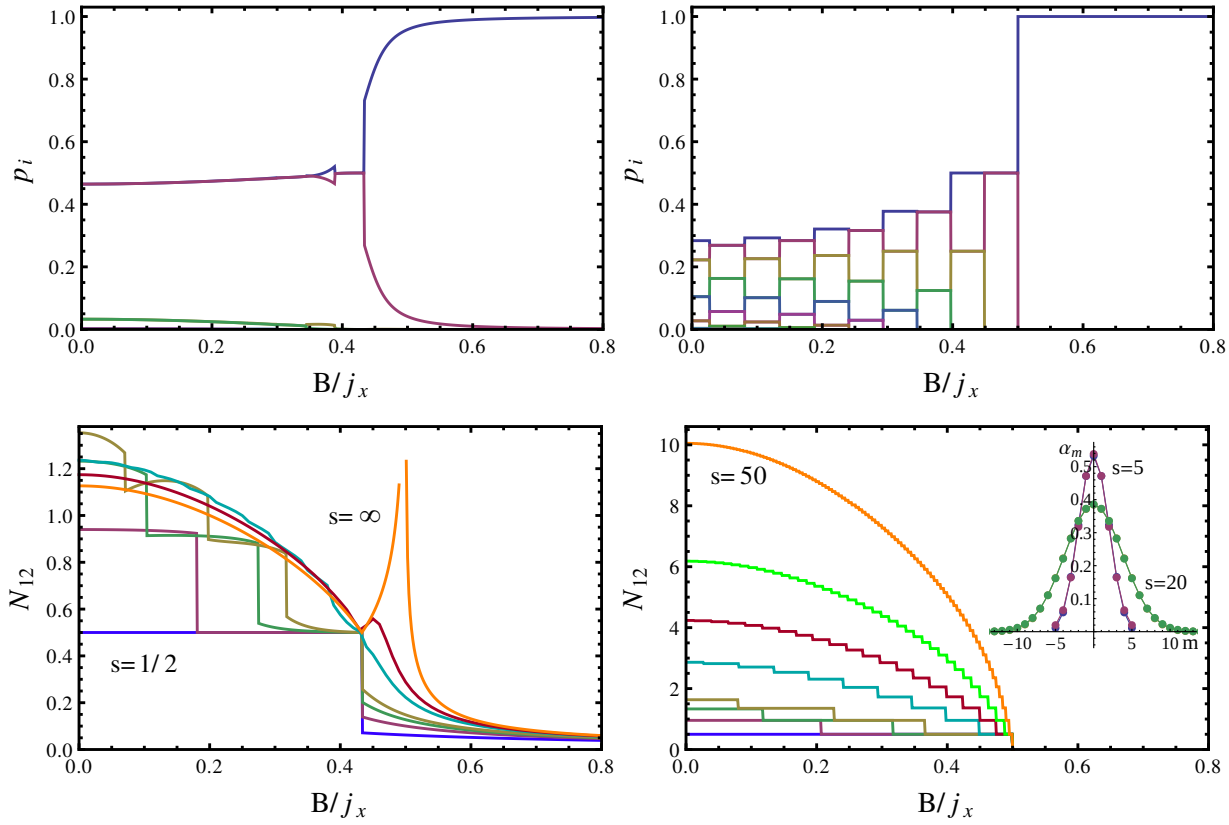

FIG. 7. (Color online) Top: The entanglement spectrum of the GS of a spin s pair as a function of the applied field for $s = 5$ and $\chi = J_y/J_x = 0.75$ (left) and 1 (right). In the anisotropic case it is formed essentially by just two degenerate eigenvalues below the factorizing field (as described by Eq. (19)), whereas in the XX case (right) there are several non-vanishing eigenvalues (two-fold degenerate), in agreement with the gaussian profile (24) (shown in the bottom right panel for $s = 5$ and 20, together with the exact results, indistinguishable from (24)). Bottom: The negativity of the pair as a function of the (scaled) magnetic field for different spin values and $\chi = 0.75$ (left), where $s = 1/2, 1, \frac{3}{2}, 2, 5, 10$ and ∞ (bosonic limit, Eq. (20)), and $\chi = 1$ (right), where $s = 1/2, 1, \frac{3}{2}, 2, 5, 10, 20$ and 50. Notice the different scales.

large s if θ is not too small, i.e., $N(|\Theta_+\rangle) = \frac{1-\cos^{4s}\theta}{2(1+\cos^{4s}\theta)}$, $N(|\Theta_-\rangle) = \frac{1}{2}$, which for $B < B_s$ lies below the exact value. The latter remains, however, *bounded as the spin s increases* if $|\chi| < 1$. Its maximum at zero field is in fact attained at low finite spin ($s \approx 2$ for $\chi = 0.75$, as seen in the bottom left panel of Fig. 7).

For large s and $\chi < 1$, the correction $|\delta\psi_\pm\rangle$ and its effect on the pair negativity and entanglement entropy can be determined through a bosonic RPA approach [29]. Around

the normal mean field phase ($B > B_c = J_x s$) such approach implies at lowest order the replacements $S_i^z \approx b_i^\dagger b_i - s$, $S_i^+ \approx b_i^\dagger$, $S_i^- \approx b_i$ with b_i, $b_i^\dagger$ bosonic operators ($[b_i, b_j^\dagger] = \delta_{ij}$), while around the parity-breaking mean field a similar replacement is to be applied to the rotated spin operators $S_i^{z'}$, $S_i^{\pm'}$, with $S_i^{-'}|\Theta\rangle = 0$. Taking into account parity restoration effects, such bosonisation leads to the analytic expression

$$N_{12} = \begin{cases} f + \sqrt{f(f+1)}\,, & |B| > B_c = J_x s \\ 2[f + \sqrt{f(f+1)}] + 1/2\,, & |B| < B_c \end{cases} \tag{20}$$

where f is the average single site bosonic occupation number,

$$f = \tfrac{1}{2}(\sqrt{1 + \tfrac{\lambda^2 - \omega_m^2}{\omega_+ \omega_-}} - 1)\,, \tag{21}$$

with $\lambda = |B|$ (B_c) for $|B| > B_c$ ($< B_c$), $\omega_m = \frac{\omega_+ + \omega_-}{2}$ and $\omega_\pm$ the bosonic eigenfrequencies

$$\omega_\pm = \begin{cases} B_c\sqrt{(1 \pm (B/B_c)^2)(1 \pm \chi)}\,, & |B| < B_c \\ B_c\sqrt{(B/B_c \pm 1)(B/B_c \pm \chi)}\,, & |B| > B_c \end{cases}\,. \tag{22}$$

The exact results for the negativity are verified to approach the previous finite and s-independent bosonic limit for large spin in the anisotropic case $\chi < 1$ (bottom left panel in Fig. 7). The corresponding pair entanglement entropy is given by $S_2 = -f \log_2 f + (f + 1)\log_2(f+1) + \delta$, where $\delta = 0$ (1) for $B > B_c$ ($< B_c$) [29].

However, in the XX case $\chi = 1$ ($J_y = J_x$) the behavior for high spin is different. Here H_{12} commutes with the total spin component $S_t^z = S_1^z + S_2^z$, implying that the parity breaking solution of the pair mean field is actually breaking a continuous symmetry. Symmetry restoration implies then integration over all rotations around the z axis (i.e., projection onto definite magnetization) and the previous approach (Eqs. (19)–(20)) no longer holds. Nevertheless, since the exact GS has now definite magnetization M, it is of the form

$$|\psi_M\rangle = \sum_{m=-s}^{M+s} \alpha_M^m |m, M-m\rangle\,, \quad (\chi = 1) \tag{23}$$

for $M \leq 0$, with M determined by the applied transverse field ($M \approx -2s[B/B_c]$ for $B \leq B_c$, $[\ldots]$ integer part) and all α_M^m of the same sign for $J_x > 0$ in (1). Eq. (23) is directly its Schmidt decomposition, implying that the single spin reduced state will have eigenvalues $|\alpha_M^m|^2$, two-fold degenerate for $m \neq M/2$ ($\alpha_M^m = \alpha_M^{M-m}$), leading to the entanglement spectrum of the top right panel in Fig. 7. The number of non-zero eigenvalues (the Schmidt

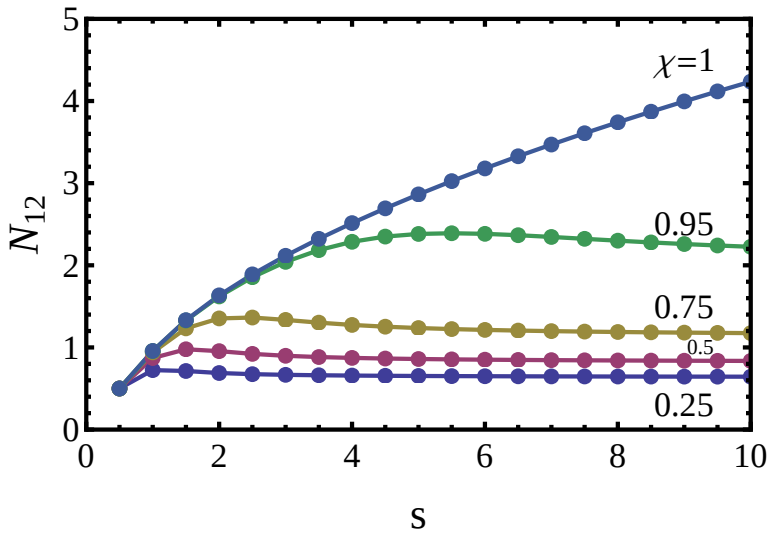

FIG. 8. (Color online) Negativity of a pair for increasing spin s at zero field for different anisotropies $\chi = J_y/J_x$. For $\chi < 1$ they saturate, approaching the limit values (20), while for $\chi = 1$ they increase as $\sqrt{s}$, as given by Eq. (25) (indistinguishable from the exact result for $s \geq 1$ on this scale).

rank of $|\psi_M\rangle$) will then be $2s + 1 - |M|$. For $|M|$ not too close to $2s$ the coefficients will have essentially a *gaussian distribution*, as appreciated in the bottom right panel of Fig. 7,

$$\alpha_M^m \propto e^{-(m-M/2)^2/(4\sigma_M^2)}, \quad \sigma_M \approx r_M s \tag{24}$$

where for s not too small, the fluctuation $\sigma_M^2 \approx \langle (S_1^z - M/2)^2 \rangle$ will be *proportional to the spin* s, as obtained from the high spin expansion of the exact eigenvector equation. The factor r_M decreases for increasing $|M|$ and for $M = 0$ it is given by $r_0 = 1/(2\sqrt{2}) \approx 0.35$, whereas for $|M| = s/2$, $r_{s/2} \approx 0.32$. The overlap between the gaussian expression and exact distribution exceeds 0.999 for $s \geq 5$ at $M = 0$.

Let us remark that for two spins s coupled to total spin $2s$ and magnetization M, the corresponding distribution of the α_M's are Clebsch-Gordan coefficients, which also lead to a gaussian distribution for high s and $|M|$ not close to $2s$, with a width also proportional to s but slightly smaller (at zero field, $\sigma_0^2 \approx s/4 < s/(2\sqrt{2})$). Hence, the actual distribution in the GS of the XX pair contains small admixtures from lower values of the total spin, as H_{12} does not commute with it.

Therefore, the negativity of the pair can be estimated through the gaussian approxima-

tion, which leads, using Eq. (9), to

$$N_{12} \approx \sqrt{2\pi\sigma_M^2} - \tfrac{1}{2} \approx \sqrt{2\pi r_M s} - \tfrac{1}{2}\,. \tag{25}$$

Consequently, the entanglement is *unbounded* for increasing spin, with N_{12} increasing as $\sqrt{s}$ for $\chi = 1$, as verified in the bottom right panel of Fig. 7 and in Fig. 8. The entanglement entropy of the pair becomes, similarly, $S(\rho_1) \approx \frac{1}{2\ln 2}[1 + \ln(2\pi\sigma_M^2)] \approx \frac{1}{2\ln 2}[1 + \ln(2\pi r_M s)]$.

The previous behavior of the pair entanglement with s holds also for an XXZ coupling $-J(S_1^x S_2^x + S_1^y S_2^y) - J_z S_1^z S_2^z$ if $J_z > -J$ ($J > 0$), in which case the coefficients α_M^m remain gaussian with finite width σ_M. However, in the AFM case $J_z = -J$, $J > 0$ (equivalent through local rotations to $J_z = J < 0$) at zero magnetization, the gaussian becomes uniform and the pair GS becomes *maximally entangled*, i.e. $|\alpha_m^0| = 1/\sqrt{2s+1}\ \forall\ m$ (with $|\psi_0\rangle$ becoming the singlet state with zero total angular momentum for $J_z = J < 0$). Such state leads then to $N_{12} = s$ and $S(\rho_1) = \log_2(2s{+}1)$, with maximum fluctuation $\langle S_1^{z\,2}\rangle = s(s{+}1)/3$.

IV. CONCLUSIONS

We have analyzed the behavior of pair entanglement and magnetization in dimerized spin-s chains with XY couplings in a transverse field. It was shown that for weak coupling between pairs, these quantities can be correctly described by a self-consistent pair mean field approach, which can predict up to $2s$ dimerized phases below the factorizing field if α is sufficiently low and $\chi > 0$, lying between S_z parity breaking phases. The dimerized sectors are visible through the concomitant approximate plateaus in the chain magnetization and pair negativity N_{12} and the low values of the pair entanglement S_2 with the rest of the chain, while the intermediate parity breaking phases through the minima in N_{12} and maxima in S_2, together with the linear increase in the magnetization. These effects can be all described by the pair mean field approach if basic parity restoration is employed in parity breaking phases. Magnetization was also seen to correlate with the entanglement entropy S_1 of a single spin, which is larger than S_2 except in the vicinity of $B < B_s$, indicating dimerization. These multiple phases arise below increasingly lower values of the coupling between pairs as s increases, with the XX case being more favorable. Non-monotonous magnetic behavior of N_{12} and S_2 nevertheless subsists for higher couplings, in agreement with the non-monotonicity of the parity breaking parameter of the pair mean field.

It was also shown that the isolated pair negativity rapidly saturates as s increases in the anisotropic XY case, in agreement with the predictions of a mean field plus RPA treatment with parity restoration, whereas in the XX case it increases as $s^{1/2}$, following a gaussian description, being then intermediate between the XY and the full AFM case.

These results show that interesting phases with non-trivial entanglement and magnetic properties can arise for non-homogeneous couplings, leading to regimes still far from the bosonic-like large s limit. Generalized self consistent mean field treatments based on non-trivial units like pairs or clusters can provide a good description of such systems in these regimes, specially if supplemented with symmetry restoration, offering a convenient starting point for more complex treatments.

The authors acknowledge support from CONICET (AB, NC, JMM), and CIC (RR) of Argentina.

---

[1] L. Amico, R. Fazio, A. Osterloh, V. Vedral, Rev. Mod. Phys. **80**, 517 (2008).

[2] J. Eisert, M. Cramer, M.B. Plenio, Rev. Mod. Phys. **82**, 277 (2010).

[3] T. J. Osborne, M.A. Nielsen, Phys. Rev. A **66**, 032110 (2002).

[4] G. Vidal, J.I. Latorre, E. Rico, A. Kitaev, Phys. Rev. Lett. **90**, 227902 (2003).

[5] M.A. Nielsen, I.L. Chuang, *Quantum Computation and Quantum Information* (Cambridge Univ. Press, Cambridge, UK, 2000).

[6] S. Haroche, J.M. Raimond *Exploring the Quantum* (Oxford, Univ. Press, Oxford, UK (2006).

[7] D. Porras, J.I. Cirac, Phys. Rev. Lett. **92**, 207901 (2004).

[8] I.M. Georgescu, S. Ashhab, and F. Nori, Rev. Mod. Phys. **86**, 153 (2014).

[9] R. Blatt and C.F. Roos, Nat. Phys. **8**, 277 (2012).

[10] C. Senko, P. Richerme, J. Smith, A. Lee, I. Cohen, A. Retzker, C. Monroe, Phys. Rev. X **5**, 021026 (2015).

[11] R. Barends et al Nature **534** 222 (2016); R. Barends et al Phys. Rev. Lett. **111**, 080502 (2013).

[12] M. Lewenstein, A. Sanpera, V. Ahufinger, *Ultracold Atoms in Optical Lattices*, Oxford Univ. Press, UK, 2012.

[13] J.H.H. Perk, H.W. Capel, M.J. Zuilhof, Th.J. Siskens, Phys. A **81**, 319 (1975); Th.J. Siskens, H.W. Capel, J.H.H. Perk, Phys. Lett. A **53**, 21 (1975).

[14] J.H.H. Perk, H.W. Capel, Th.J. Siskens, Phys. A **89**, 304 (1977); J.H.H. Perk, H.W. Capel, Phys. A **92**, 163 (1978); J.H.H. Perk, H. Au-Yang, J. Stat. Phys. **135**, 599 (2009).

[15] E.I. Kutznetsova, E.B. Fel'dman, JETP. Lett. **102**, 882 (2006); E.B. Fel'dman, M.G. Rudavets, JETP. Lett. **81**, 47 (2005). S.I. Doronin, A.N. Pyrkov, E.B. Fel'dman,, JETP Lett. 85, 519 (2007).

[16] C.K. Majundar, D.K. Gosh, J. Math. Phys. **10**, 1388 (1969); *ibid* **10**, 1399 (1969); B.S. Shastry and B. Sutherland, Phys. Rev. Lett. **47**, 964 (1981).

[17] H.J. Schmidt, J. Phys. A **38** 2123 (2005).

[18] D. Kaszlikowski, W. Son, V. Vedral, Phys. Rev. A **76**, 054302 (2007).

[19] M.-G. Hu, K. Xue, M.-L. Ge, Phys. Rev. A **78**, 052324 (2008).

[20] J. Sirker, A. Herzog, A.M. Oles, P. Horsch, Phys. Rev. Lett. **101** 157204 (2008); A. Herzog, P. Horsch, A.M. Oles, J. Sirker, Phys. Rev. B **84** 134428 (2011).

[21] P. Merchant, B. Normand, K.W. Kramer, M. Boehm, D.F. McMorrow, Ch. Regg, Nature Phys. **10**, 373 (2014).

[22] G.L. Giorgi, Phys. Rev. B **79**, 060405(R) (2009); **80**, 019901(E)(2009).

[23] N. Canosa, R. Rossignoli, J.M. Matera, Phys. Rev. B **81**, 054415 (2010).

[24] A. Boette, R. Rossignoli, N. Canosa, J.M. Matera, Phys. Rev. B **91**, 064428 (2015).

[25] C.A. Lamas, J.M. Matera, Phys. Rev. B**92**, 115111 (2015); J.M. Matera, C.A. Lamas, J. Phys.: Condens. Matter **26** 326004 (2014).

[26] V. Ohanyan, O. Rojas, J. Strečka, S. Bellucci, Phys. Rev. B **92**, 214423 (2015).

[27] T. Ramos, H. Pichler, A.J. Daley, P. Zoller, Phys. Rev. Lett. **113**, 237203 (2014). A.W. Glaetzle, M. Damonte, R. Nath, C. Gross, I. Bloch, P. Zoller, Phys. Rev. Lett. **114** 173002 (2015); I. Bloch, J. Dalibard, W. Zwerger, Rev. Mod. Phys. **80**, 885 (2006).

[28] E. Lieb, T. Schultz, D. Mattis, Ann. Phys. **16** 407 (1961).

[29] J.M. Matera, R. Rossignoli, N. Canosa, Phys. Rev. A **82**, 052332 (2010).

[30] J. Kurmann, H. Thomas, G. Müller, Phys. **A** 112, 235 (1982).

[31] G. Vidal and R.F. Werner, Phys. Rev. A **65**, 032314 (2002).

[32] K. Zyczkowski, P. Horodecki, A. Sanpera, M. Lewenstein, Phys. Rev. A **58**, 883 (1998); K. Zyczkowski, *ibid.* **60**, 3496 (1999).

[33] R. Rossignoli, N. Canosa, J.M. Matera, Phys. Rev. A **77**, 052322 (2008).

[34] R. Rossignoli, N. Canosa, J.M. Matera, Phys. Rev. A **80**, 062325 (2009).

[35] R.F. Werner, Phys. R ev. A **40**, 4277 (1989).

[36] S. Rachel, Euro. Phys. Lett. **86**, 37005 (2009).

[37] F. Michaud, F. Vernay, S.R. Manmana, and F. Mila, Phys. Rev. Lett. **108**, 127202 (2012); M. Lajko, P. Sindzingre, and K. Penc, ibid. **108**, 017205 (2012).

[38] V. Karimipour and L. Memarzadeh, Phys. Rev. **B 77**, 094416 (2008):